GAS FLOW IN THE SOLAR NEBULA LEADING TO THE FORMATION OF JUPITER

MINORU SEKIYA and SHOKEN M. MIYAMA
Department of Physics, Kyoto University, Kyoto, Japan

and

CHUSHIRO HAYASHI
Momoyama Yogoro-cho 1, Fushimi-ku, Kyoto, Japan

(Received 23 September, 1986)

Abstract. Three-dimensional gas flow in the solar nebula, which is subject to the gravity of the Sun and proto-Jupiter, is numerically calculated by using a three-dimensional hydrodynamic code – i.e., the so-called smoothed-particle method. The flow is circulating around the Sun as well as falling into a potential well of proto-Jupiter. The results for various masses of proto-Jupiter show that (1) the e-folding growth time of proto-Jupiter by accretion of the nebular gas is as short as about 300 years in stages where the mass of proto-Jupiter is 0.2 ~ 0.5 times the present Jovian mass, and that (2) proto-Jupiter begins to push away the nebular gas from the orbit of proto-Jupiter and form a gap around the orbit, when its mass is about 0.7 times the present Jovian mass. It is possible that this pushing-away process determined the present Jovian mass.

1. Introduction

Each of the giant planets contains a rock and icy core of $10-30\ M_\oplus$ (see a review by Stevenson, 1982). This remarkable similarity of masses is consistent with the following scenario. Solid planetesimals grow by collisional coagulation in the solar nebula which itself is stable against gravitational instability. When the mass of a planetesimal exceeds $10^{24}-10^{25}$ g, the ambient nebular gas is attracted to form an atmosphere around the planetesimal. Hereafter, we call such a massive planetesimal a protoplanet and its solid region a core. When the core mass exceeds a critical value of about $10\ M_\oplus$, its atmosphere becomes unstable and contracts toward the core (Mizuno, 1980). At this time, the mass of the atmosphere is also about $10\ M_\oplus$. This critical core mass as well as the atmospheric mass scarcely depends on the distance of a protoplanet from the Sun. At the onset of above-mentioned Mizuno's instability, the sum of the core mass and the atmospheric mass is about $20\ M_\oplus$ and is much smaller than the masses of present Jupiter and Saturn.

For the further evolution of proto-Jupiter, Bodenheimer (1985) showed that, with the growth of proto-Jupiter, its envelope contracts keeping a nearly hydrostatic balance, and its mass becomes about $0.2\ M_J$ (M_J being the present Jovian mass) in a period of 5×10^4 yr. Further he showed that, afterwards, the contraction rate of the protoplanet increases so that the radius of its boundary surface becomes as small as $0.16 r_H$ (r_H being the Hill radius) in a period of 2×10^3 yr, and $0.018 r_H$ in

Earth, Moon, and Planets **39** (1987) 1–15.

7.2×10^4 yr. Bodenheimer assumed that the gas accretion is negligible in this rapid contraction stage, but the effect of accretion is to be taken into account (Safronov and Ruskol, 1982). One of the aims of this paper is to find this accretion rate.

On the other hand, evolution of the nebula itself in this accretion phase was studied by Goldreich and Tremaine (1980), and Papaloizou and Lin (1984). They developed theories based on linearized hydrodynamic equations, and deduced the transfer rate of angular momentum in the protoplanet-nebula system. Their conclusion is that a protoplanet in the solar nebula pushed away nebular gases from its orbit, opened up a gap in the nebula, and finally terminated the further accretion of gases. Another aim of this paper is to study nonlinear effects in the above process by means of numerical integration of 'fully nonlinear' hydrodynamic equations.

Previously, the numerical study of the 'nonlinear' flow around a protoplanet was performed by Miki (1982); he calculated numerically the stationary flow of a polytropic gas ($n = 1.5$) in the neighborhood of a protoplanet in the approximation of a two-dimensional flow, where the variation of physical quantities in a direction perpendicular to the nebular disk was neglected. His results showed that two trailing arms appear near the Jovian position when the proto-Jovian mass exceeds one tenth of the present Jovian mass. He did not, however, solve the flow in stages after Mizuno's instability, since his intention at the time of his calculation was mainly to find a boundary condition for the primordial atmosphere of a protoplanet (for the atmosphere, see Hayashi *et al.*, 1979).

In this paper, we calculate the three-dimensional flow of an isothermal gas which is circulating around the Sun and is, partly, falling into a potential well of proto-Jupiter under the gravitational effect of the Sun and proto-Jupiter. We consider various masses of proto-Jupiter and restrict ourselves to a region outside the photosphere of proto-Jupiter, where density is low enough and gases are transparent to visible and infrared radiation. As will be shown in Section 3, a two-arm pattern as was found by Miki appears also in the three-dimensional calculation. Further, we find that proto-Jupiter itself pushes away gases from its orbit when the mass of proto-Jupiter is as large as the present Jovian mass.

2. Basic Equations and Numerical Method

In this paper, we intend to find basic features of the nebular gas flow. For this purpose, we make the following simplifications:

(1) The Sun is at rest relative to an inertial frame.

(2) The motion of a protoplanet is Keplerian.

(3) We consider stages where the photosphere of the protoplanet has contracted to a size much smaller than (say, one fifty of) the Hill radius r_H. Here, the Hill radius is given by

$$r_H = a_p \, (M_p/3 \, M_\odot)^{1/3} = 0.355 \, (a_p/5.2 \text{ AU}) \cdot (M_p/M_J)^{1/3} \text{ AU}, \tag{2.1}$$

where a_p and M_p are the mean orbital radius and the mass of the protoplanet,

respectively. According to Bodenheimer (1985) (see Section 1), this circumstance is realized at 1.2×10^5 yr after Mizuno's instability (Bodenheimer, 1985).

(4) In our calculation, the computation time is mainly consumed by the computation of fluid particles rotating rapidly around the protoplanets. In order to save this computation time, we cut off the gravitational potential of a protoplanet at a sphere with the radius, $r_c = 0.1 r_H$, and the potential in the inner regions is approximated by a harmonic potential. That is, the gravitational force of the protoplanet is written as

$$\mathbf{F}_p(\mathbf{r}_p) = \begin{cases} -GM_p \mathbf{r}_p / r_p^3 & (r_p \geqq r_c) \\ -GM_p \mathbf{r}_p / r_c^3 & (r_p < r_c), \end{cases} \tag{2.2}$$

where $\mathbf{r}_p$ is the radial vector from the protoplanet, and r_p is the absolute value of $\mathbf{r}_p$ (hereafter, the absolute value of a vector is represented by the light-face letter). We further assume that the growth rate of the protoplanet is given by the rate of mass inflow across the sphere with the cutoff radius. We have checked that both the flow pattern outside the Hill sphere and the growth rate of the protoplanet scarcely depend on the adopted value of the cutoff radius r_c as long as $r_c \ll r_H$.

(5) Gravitational force due to the nebular gas is neglected. The effect of this force can be approximated by a very slight change of the solar gravity when the nebula is nearly axisymmetric. This assumption is valid in such a case.

(6) We assume the gas to be isothermal and use the value of temperature, T, at the orbit of the protoplanet, which is determined by the balance of heating due to solar irradiation and cooling due to radiation from grain particles floating in the nebula – i.e.,

$$T = (L_\odot / 16\pi a_p^2 \sigma)^{1/4} = 123\ (a_p / 5.2\ \mathrm{AU})^{-1/2}\ \mathrm{K}, \tag{2.3}$$

where $L_\odot$ is the solar luminosity and σ is the Stefan-Boltzmann constant. Strictly speaking, the gas temperature is not constant, that is, the equilibrium temperature decreases with the distance from the Sun and also the temperature rises if a gas element is compressed relatively rapidly. In this paper, however, we restrict ourselves only to study the basic features of the flow around the orbit of a protoplanet; thus the calculation with the above assumptions is sufficient for our purpose.

Now, we use a rotating coordinate system such that the origin is at the Sun, and that the x- and y-axes rotate around the z-axis with the mean angular velocity Ω of the protoplanet, whose mean position is on the positive x-axis. Then the equation of motion of a nebular gas element of the nebular gas is written as

$$\frac{\mathrm{D}\mathbf{v}}{\mathrm{D}t} = -2\boldsymbol{\Omega} \times \mathbf{v} - \boldsymbol{\Omega} \times (\boldsymbol{\Omega} \times \mathbf{r}) - \frac{GM_\odot \mathbf{r}}{r^3} + \mathbf{F}_p(\mathbf{r}_p) - \frac{1}{\rho} \nabla P + \mathbf{S}. \tag{2.4}$$

Definitions and notations used in this equation will be described in the following.

First, $\mathbf{v}$ is the velocity and $\mathbf{r}$ is the position vector of the gaseous element from the

Sun. Furthermore, ρ is the density and P is the pressure. They satisfy the equation of state,

$$P = kT\rho/m = c^2\rho, \tag{2.5}$$

where k is the Boltzmann constant, m is the mean molecular mass ($= 3.92 \times 10^{-24}$ g). Finally $\mathbf{S}$ is the artificial viscosity term, whose strength is adjusted so that the plane shock wave in the standard shock-tube problem is well reproduced.

In order to integrate, Equation (2.4), we use a Lagrangian hydrodynamic code, i.e., the so-called smoothed particle method, details of which will be described in Miyama *et al.* (1986). The number of particles used in our computation is about 30000. All the particles have the same mass, 2×10^{26} g. The size of a particle is inversely proportional to the cubic root of the local gas density. For instance, the initial size of the particle at the Jovian orbit is 0.14 AU and the spatial resolution of the computation is limited to the order of this size. We integrate the equation of motion of each particle by the Runge-Kutta-Gill method in the fourth order.

For each model of our calculation, the particles are initially distributed with the surface density distribution given by Hayashi (1981):

$$\rho_s = 1.4 \times 10^2 \ (a/5.2 \text{ AU})^{-3/2} \text{ g cm}^{-2}, \tag{2.6}$$

where a is the equatorial distance from the Sun, i.e., $a = (x^2 + y^2)^{1/2}$. Then the density distribution is written as

$$\rho = 1.5 \times 10^{-11} \ (a/5.2 \text{ AU})^{-3} \exp(-(z/H)^2) \text{ g cm}^{-3}, \tag{2.7}$$

where H ($= 2^{1/2}c/\Omega$) is the vertical scale height.

We assume that initially each fluid element is in a circular motion around the Sun, where the velocity in the present rotating frame is determined by the balance of the solar gravity, the pressure force and the centrifugal force: namely, the components of the initial velocity in the cylindrical coordinates (a, ϕ, z) are given by

$$v_\phi = \Omega a\{(a_p^3/a^3 - 3(c/\Omega a)^2)^{1/2} - 1\}, \tag{2.8}$$

and

$$v_a = v_z = 0, \tag{2.9}$$

where we have neglected terms on the order of $(c/v_K)^4 \sim 10^{-5}$, where v_K is the mean Keplerian velocity of the protoplanet.

The calculation is made for a cylindrical region, $0.53a_p \leqq a \leqq 1.47a_p$, which is enclosed by smooth and rigid boundaries. In regions just inside and outside the inner and outer boundaries, respectively, we put about 5000 particles whose densities and velocities are always given by Equations (2.7), (2.8), and (2.9) and which play a role of exerting pressure force on particles in the cylindrical region considered. Owing to economic circumstances our calculation was terminated at $2t_K$ for each model, where t_K is the Keplerian period of the protoplanet.

TABLE I

Parameters used for each model, a_p: mean ortital radius, e: eccentricity, M_p: mass of a protoplanet. Gas accretion time, $M_p/\dot{M}$ ($\dot{M}$ being gas accretion rate) and number of figure are also listed. Only in model E, the x- and y-components of the pressure force are neglected.

Model	a_p (AU)	e	$M_p/M_\odot$	M_p/M_J	$M_p/\dot{M}$ (yr)	Figure
A	5.2	0	2.5×10^{-4}	0.26	2.6×10^2	1
B	5.2	0	5.0×10^{-4}	0.52	2.6×10^2	2
C	5.2	0	1.0×10^{-3}	1.04	3.1×10^2	3
D	5.2	0	2.0×10^{-3}	2.09	3.5×10^2	4
E	5.2	0	2.5×10^{-4}	0.26	1.9×10^2	5
F	5.2	0.05	2.5×10^{-4}	0.26	2.5×10^2	8
G	5.2	0.05	1.0×10^{-3}	1.04	3.5×10^2	10
H	9.5	0	2.5×10^{-4}	0.26	1.9×10^2	11
I	9.5	0.05	2.5×10^{-4}	0.26	2.1×10^2	12

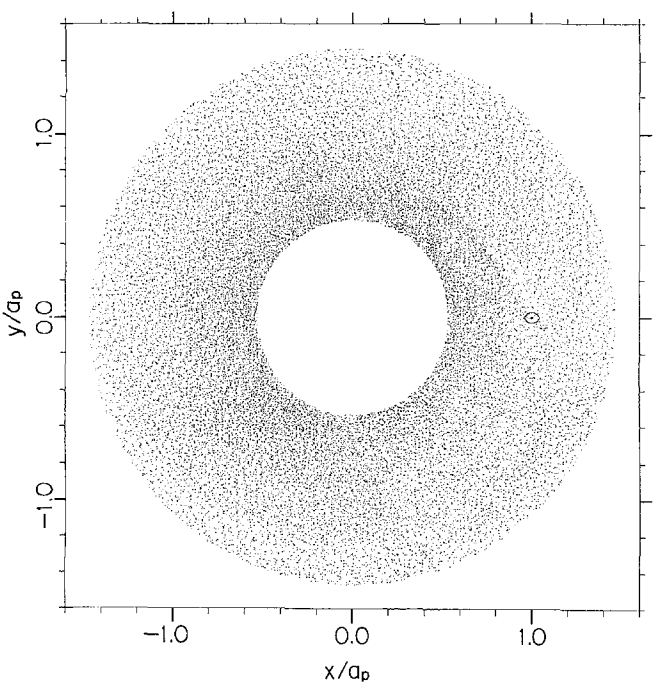

Fig. 1. Postitions of the centers of 30000 fluid elements projected onto the equatorial plane of the nebula (the x–y plane) for model A: $a_p = 5.2$ AU, $e = 0$, $M_p = 0.26\ M_J$ and $t = 1.75\ t_K$. The Hill sphere of the protoplanet is also shown

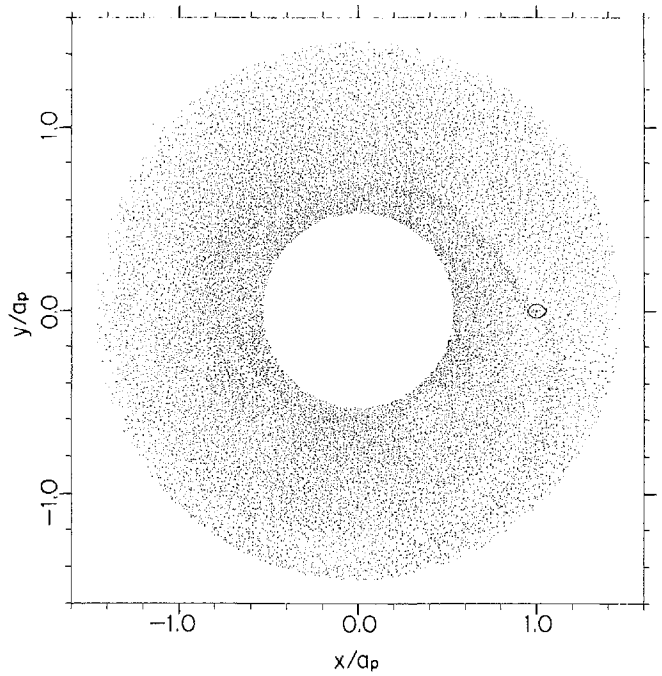

Fig. 2. Model B: $a_p = 5.2$ AU, $e = 0$, $M_p = 0.52\ M_J$ and $t = 1.75\ t_K$.

3. Results and Discussion

A model of the gas flow is characterized by the mean orbital radius, a_p, eccentricity, e, and mass, M_p, of the protoplanet. Values of these parameters adopted for numerical calculations are listed in Table I. Only in model E, the x- and y-components of pressure force have been neglected in order to see the pressure effect on the flow. In each model, calculation is performed for a period of $2t_K$ with the initial condition described in the previous section. The growth time of the protoplanet is calculated from the amount of gases trapped within a sphere of the cutoff radius r_c during this period.

It is to be noticed that the growth time listed in Table I is meaningful only when the mass of proto-Jupiter is smaller than, say, 0.5 M_J for the following reason. In our calculation, we have adopted for all the models the initial density distribution given by Equation (2.7) without taking into account the evolution of the nebula until proto-Jupiter has grown to the masses listed in Table I. In reality, the density of nebular gases around the orbit of proto-Jupiter is reduced considerably when the mass of proto-Jupiter is about the present Jovian mass (see Figure 3).

Figures 1–5, 8, and 10–12 show the projection of the centers of all the fluid elements onto the $x-y$ plane at $t = 1.75t_K$. Further, choosing model C as an example, we show in Figure 6 the pattern of flow velocity in the neighborhood of the

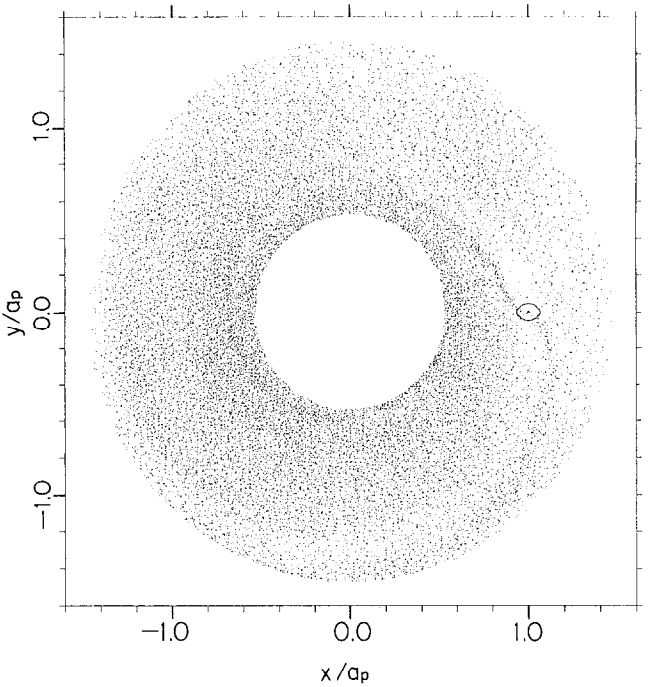

Fig. 3. Model C: $a_p = 5.2$ AU, $e = 0$, $M_p = 1.04\ M_J$ and $t = 1.75 t_K$.

protoplanet at $t = 1.75 t_K$. It is seen that the orbit of most of the gaseous elements, which are dragged by the gravity of the protoplanet, is turned by the Coriolis force to pass over to the other side of the protoplanetary orbit. Only a very small fraction of the elements falls into the sphere with the cutoff radius; these elements have counterclockwise orbital angular momenta around the protoplanet. The flow velocity patterns in the other models are similar to that of model C.

Now, we first compare models A, B, C, and D. In these models, the orbital radius of the protoplanet is fixed to the present Jovian value, and the protoplanetary masses are about 1/4, 1/2, 1 and 2 times the present Jovian mass, M_J ($= 9.54 \times 10^{-4}\ M_\odot$), respectively. Two trailing arms extending from the position of proto-Jupiter are clearly seen for the case of $M_p \gtrsim 1\ M_J$ (see Figures 3 and 4 as compared with Figures 1 and 2). That is, nebular gases are pushed away from the orbit of proto-Jupiter and a ring-like void region is formed.

In order to understand the reason why such a pattern appears for $M_p \gtrsim 1\ M_J$, we compare the result of model A with that of a test computation where M_p is the same and is as small as $0.26\ M_J$, but the x- and y-components of the pressure force are put equal to zero (model E, see Figure 5). In model E, the two-arm structure with the ring-like void is clearly seen as in model D. This shows that clear patterns do not appear in models A and B because the pressure effect of the nebula overcomes the gravitational effect of the protoplanet and, hence, the density contrast is reduced greatly.

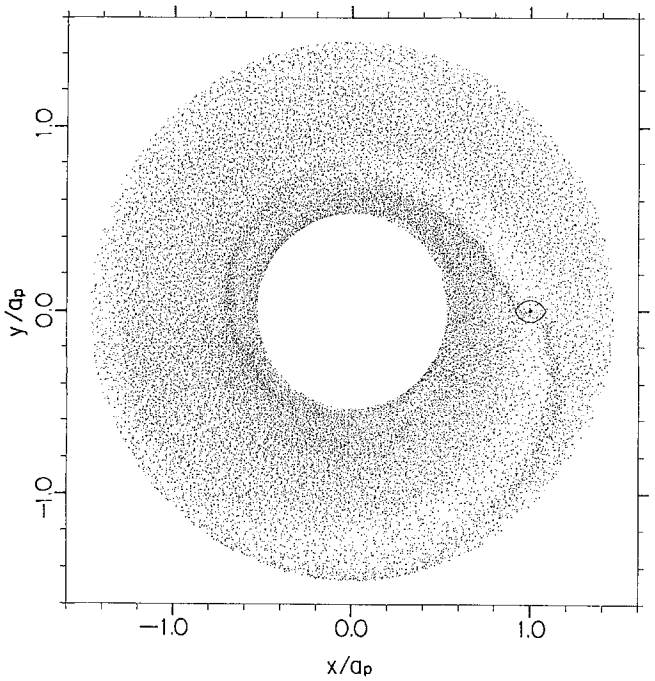

Fig. 4. Model D: $a_p = 5.2$ AU, $e = 0$, $M_p = 2.09\ M_J$ and $t = 1.75 t_K$.

For comparison, we show in Figure 7 the orbits of test particles moving under the gravity of the Sun and a protoplanet alone, i.e., the orbits in the so-called circular restricted three-body problem. This figure has been taken from Nishida (1983). The arm pattern found in models C, D, and E (Figures 3–5) appears just in regions in Figure 7 where the orbits of test particles intersect with each other. This is interpreted as that the fluid elements cannot intersect with each other so that density rises abruptly when fluid elements collide with each other. It is to be noticed that, even in model E where the x- and y-components of the pressure force are neglected, the orbit of a fluid element is different from that of a test particle, since in our numerical calculation the artificial viscosity term **S** operates.

Now, we consider a condition for the formation of the ring-like void and the arm pattern. The region where the gravitational force of the protoplanet is more effective than that of the Sun is the interior of the Hill sphere with the radius, r_H. The pressure effect travels over the distance r_H in a time, $\tau_{pr} = r_H/c$. On the other hand, a fluid element passes through the Hill sphere in a time on order of $\tau_K = 1/\Omega$. Then, the criterion for the ineffectiveness of the pressure is given by $\tau_K \lesssim \tau_{pr}$, that is, $c \lesssim r_H\Omega$. Using the temperature given by Equation (2.3), we can rewrite the criterion as

$$M_p \gtrsim 0.4\ (a_p/5.2\ \text{AU})^{3/4} M_J. \tag{3.1}$$

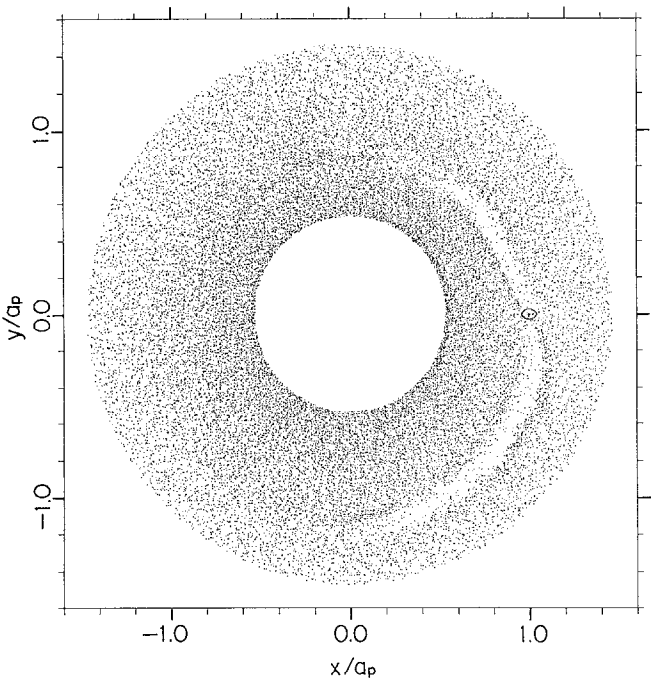

Fig. 5. Model E: $a_p = 5.2$ AU, $e = 0$, $M_p = 0.26\ M_J$ and $t = 1.75 t_K$. The x- and y-components of the pressure force are neglected.

This criterion agrees with the numerical results for models A to D within a factor 2, although we make rough estimate of the order of magnitude.

The above results show that proto-Jupiter itself pushed away the gases lying in its feeding zone, i.e., a belt zone around the orbit of proto-Jupiter, where accreting gases were circulating. From our numerical results, we find that this pushing-away process becomes effective when the mass of proto-Jupiter exceeds about 0.7 M_J. We can consider that, when the mass of proto-Jupiter becomes equal to that of present Jupiter, the accretion of the nebular gas onto proto-Jupiter stops and hereafter it evolves as an isolated system. The Helmholtz-Kelvin contraction of such a system was studied by Bodenheimer *et al.* (1980), Graboske *et al.* (1975), and Grossman *et al.* (1980).

Next, in order to find the effect of the eccentric motion of proto-Jupiter on the gaseous flow, we compare cases where the eccentricities are 0 and 0.05, although the precise value of the eccentricity of proto-Jupiter is not well known. First, we consider the cases where M_p is 0.26 M_J (models A and F, see Figures 1 and 8, respectively). In the case of $e = 0$, faint arm structure can be seen in both sides of the Jovian orbit while, in the case of $e = 0.05$, the arm in the region $y > 0$ is clear but the arm in the region $y < 0$ is faint. This effect of the eccentric motion is explained as follows. In model F, ea_p ($= 0.05\ a_p$) is greater than r_H ($= 0.044 a_p$) and, as shown in Figure 9, when the protoplanet is at the perihelion, a nebular gas element which is affected by

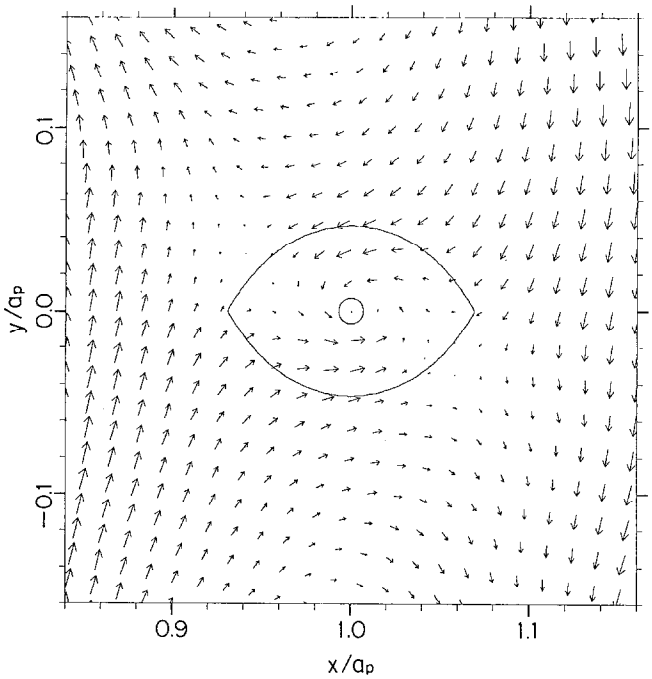

Fig. 6. Flow velocity in the equatorial plane of the nebular gas in model C. The Hill sphere and the sphere with the cutoff radius r_c are also shown.

the protoplanet comes from the region with $y < 0$. Thus the accretion column is formed only in the region $y > 0$ and, hence, the one-arm structure is formed.

On the other hand, in the case where $M_p = 1.04\, M_J$ (models C and G, see Figures 3 and 10, respectively), a similar two-arm structure appears in the both cases of $e = 0$ and 0.05. In model G, a nebular gas element which is affected by the protoplanet comes from the both regions, $y > 0$ and $y < 0$, even at the perihelion since we have ea_p ($= 0.05a_p$) $< r_H$ ($= 0.07a_p$) and, hence, the flow pattern for $e = 0.05$ resembles that for $e = 0$ (model C). Consequently, the above conclusion that proto-Jupiter pushed away gases in its feeding zone when it grew up to the present Jovian mass is not altered even if we take into account the effect of eccentricity.

For comparison, we also made calculation for Saturn's region. We studied the cases where $M_p = 0.26\, M_J$ and $e = 0$ and 0.05 (models H and I; see Figures 11 and 12, respectively). In the both cases, we cannot see a clear pattern like models C and D for proto-Jupiter. This is consistent with the criterion given by condition (3.1) for $a_p = 9.5$ AU. That is, for $M_p \lesssim 0.6\, M_J$, the pressure effect overcomes the gravitational effect and smooths out the density contrast. Therefore the above-mentioned pushing-away process cannot stop the growth of proto-Saturn when its mass becomes equal to the present Saturn mass ($0.30\, M_J$). The only process that can stop the growth of proto-Saturn is probably the escape of the nebular gases themselves from the region considered. The formation time of the Saturn core with

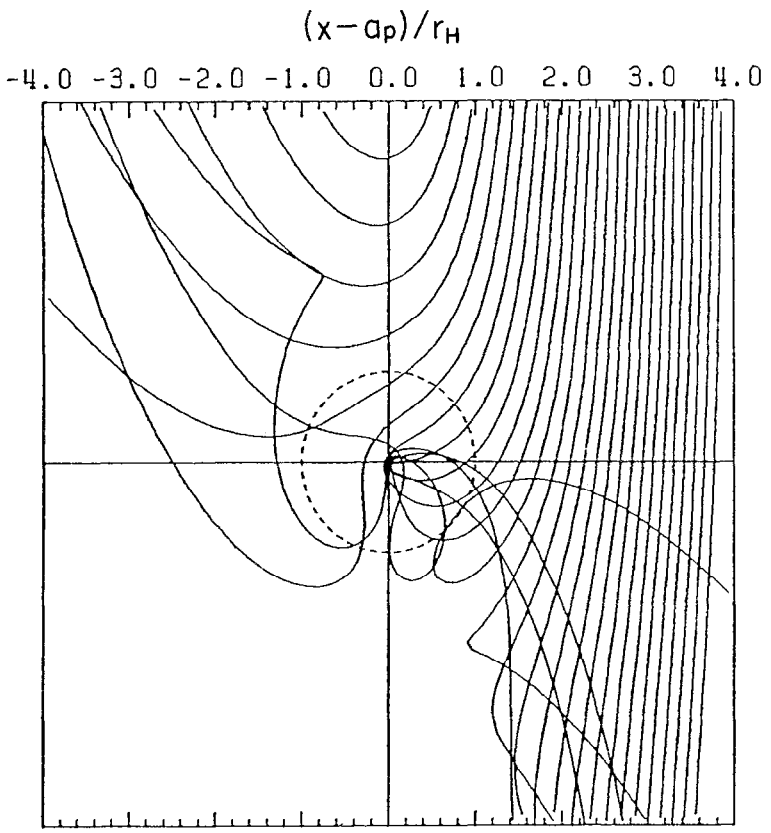

Fig. 7. Orbits of test particles moving under the gravity of the Sun and planet (taken from Nishida, 1983).

10 $M_\oplus$ in the solar nebula is several times as long as that of the Jovian core (Hayashi *et al.*, 1977; Nakano, 1986). Thus, it is possible that a considerable amount of the nebular gases in Saturn's feeding zone had been blown off before proto-Saturn reached the stage of Mizuno's instability (Hayashi *et al.*, 1985).

4. Conclusions

We calculated numerically the three-dimensional gas flow in the solar nebula circulating under the gravity of the Sun and proto-Jupiter, under the assumption that the self-gravity of the nebula is negligible and that the gas is isothermal. We obtain the following results:

(i) The e-folding growth time of proto-Jupiter is as short as 300 yr in stages where its mass is $0.2 \sim 0.5$ times the present Jovian mass, i.e., in stages where the photosphere of proto-Jupiter has already contracted within a sphere with a radius smaller than one tenth of the Hill sphere.

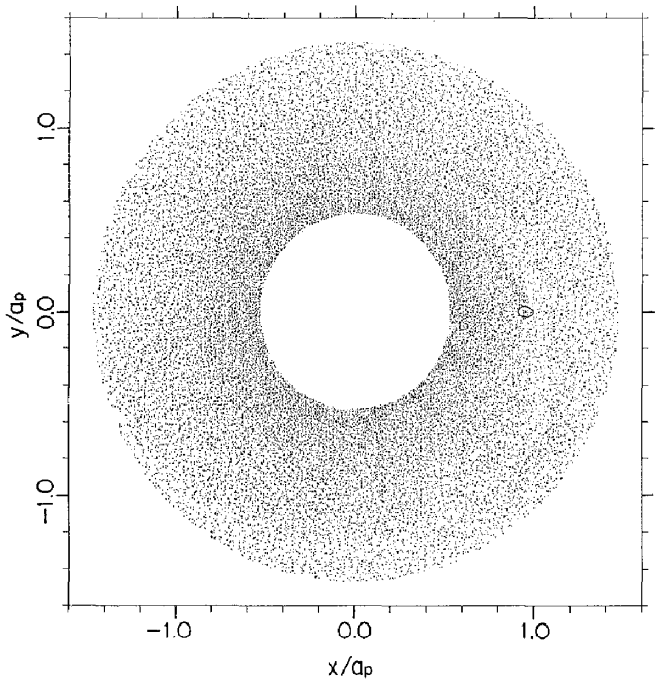

Fig. 8. Model F: $a_p = 5.2$ AU, $e = 0.05$, $M_p = 0.26\,M_J$ and $t = 1.75 t_K$. The protoplanet is at the perihelion.

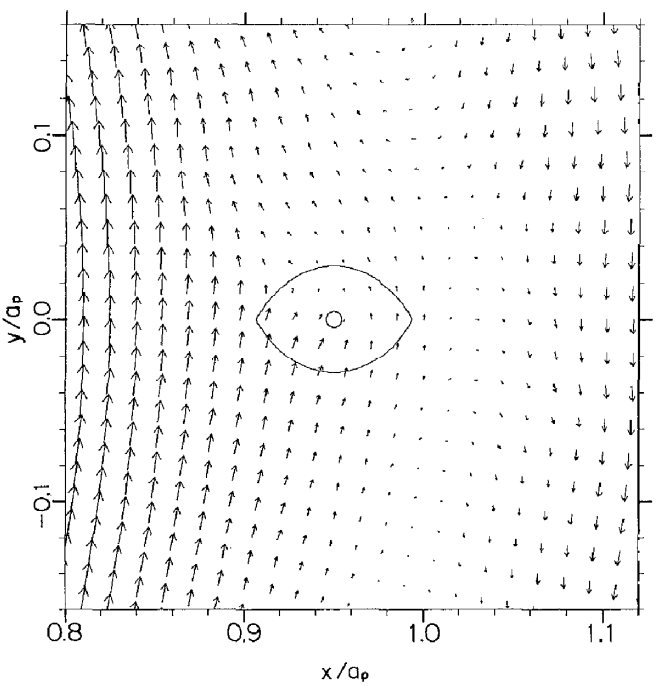

Fig. 9. Flow velocity of the nebular gas in model F. The Hill sphere and the sphere with the radius r_c are also shown.

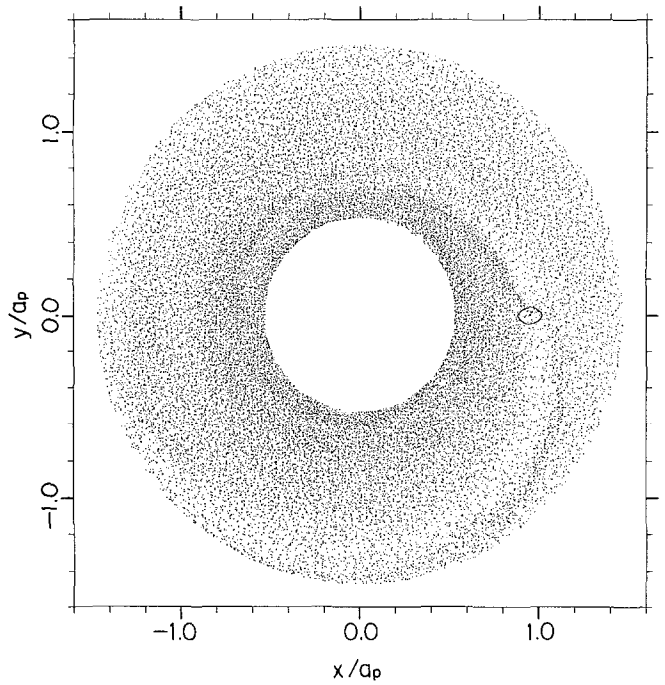

Fig. 10. Model G: $a_p = 5.2$ AU, $e = 0.05$, $M_p = 1.04\ M_J$ and $t = 1.75 t_K$. The protoplanet is at the perihelion.

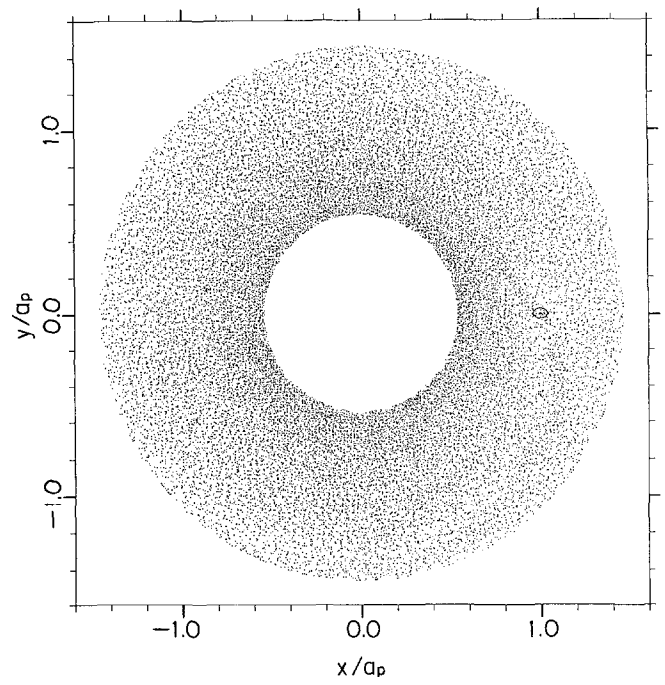

Fig. 11. Model H: $a_p = 9.5$ AU, $e = 0$, $M_p = 0.26\ M_J$ and $t = 1.75 t_K$.

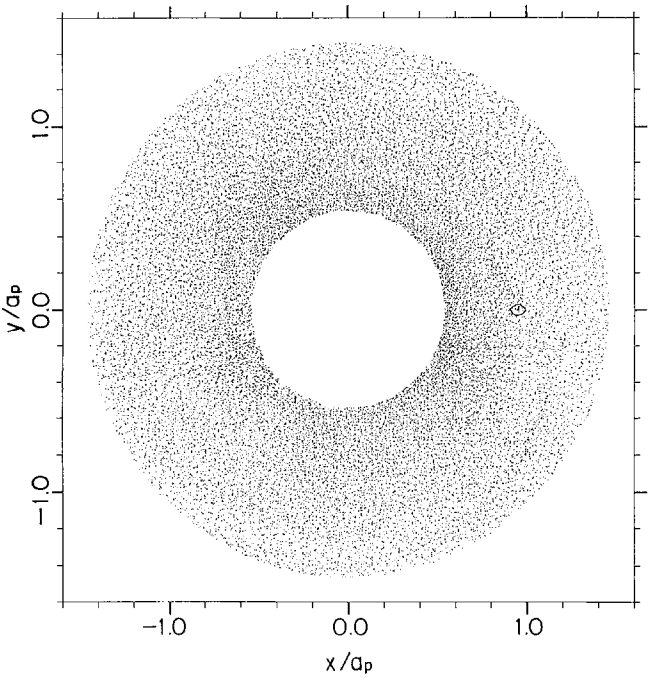

Fig. 12. Model I: $a_p = 9.5$ AU, $e = 0.05$, $M_p = 0.26\ M_J$ and $t = 1.75 t_K$. The protoplanet is at the perihelion.

(ii) When the mass of proto-Jupiter becomes about 0.7 times the present Jovian value, proto-Jupiter begins to push away gases from its orbit and form a gap around the orbit. It is considered that this process determined the present Jovian mass. This result does not depend on the eccentricity e of the orbit as far as $e \lesssim 0.05$.

(iii) The reason why the present mass of Saturn is much smaller than that of Jupiter is probably that the core formation time of Saturn was longer than that of Jupiter and a considerable amount of the nebular gases had escaped before proto-Saturn reached the stage of Mizuno's instability.

It is desired in the future to perform a numerical simulation of the simultaneous evolution of proto-Jupiter and the nebula. In this simulation, we have to take into account complex but important processes in the gas flow, such as the energy transfer by radiation and convection and the angular momentum transfer by turbulent viscosity.

Acknowledgements

Dr. Nishida kindly sent us a copy of his figure. Numerical computations were carried out by FACOM VP200 at the Data Processing Center of Kyoto University, by FACOM M200 at Nobeyama Radio Observatory, University of Tokyo, and by FACOM M382 at the Institute of Space and Astronomical Science. This work was

supported by Grant-in-Aids for Scientific Research (60300013) and for Encouragement of Young Scientists (61740140) of the Ministry of Education, Science and Culture of Japan.

References

Bodenheimer, P.: 1985, in D. C. Black, and M. S. Matthews (eds.), *Protostars and Planets II,* Univ. Arizona Press, p. 873.

Bodenheimer, P., Grossman, A. S., DeCampli W. M., Marcy, G., and Pollack, J. B.: 1980, *Icarus* **41**, 293.

Goldreich, P. and Tremaine, S.: 1980, *Astrophys. J.* **241**, 425.

Graboske, H. C. Jr., Pollack, J. B., Grossmann, A. S., and Olness, R. J.: 1975, *Astrophys. J.* **199**, 265.

Grossman, A. S., Pollack, J. B., Reynolds, R. T., Summers, A. L., and Graboske, H. C. Jr.: 1980, *Icarus* **42**, 358.

Hayashi, C.: 1981, *Prog. Theor. Phys. Suppl.* **70**, 35.

Hayashi, C., Nakazawa, K., and Adachi, I.: 1977, *Publ. Astron. Soc. Japan* **29**, 163.

Hayashi, C., Nakazawa, K., and Mizuno, H.: 1979, *Earth Planet. Sci. Lett.* **43**, 22.

Hayashi, C., Nakazawa, K., and Nakagawa, Y.: 1985 in D. C. Black and M. S. Matthews (eds.), *Protostars and Planets II*, Univ. Arizona Press, p. 1100.

Miki, S.: 1982, *Prog. Theor. Phys.* **67**, 1053.

Miyama, S., Sekiya, M., Narita, S., and Hayashi, C.: 1986, in preparation.

Mizuno, H.: 1980, *Prog. Theor. Phys.* **64**, 544.

Nakano, T.: 1986, *Monthly Notices Roy. Astron. Soc.,* in press.

Nishida, S.: 1983, *Prog. Theor. Phys.* **70**, 93.

Papaloizou, J. and Lin, D. N. C.: 1984, *Astrophys. J.* **285**, 818.

Safronov, V. S. and Ruskol, E. L.: 1982, *Icarus* **49**, 284.

Stevenson, D. J.: 1982, *Ann. Rev. Earth Planet. Sci.* **10**, 257.